Effect of synaptic plasticity on the structure and dynamics of disordered networks of coupled neurons

M. Bayati and A. Valizadeh
Institute for Advanced Studies in Basic Sciences, P.O. Box 45195-1159, Zanjan, Iran
(Received 14 March 2012; revised manuscript received 8 June 2012; published 24 July 2012)

In an all-to-all network of integrate-and-fire neurons in which there is a disorder in the intrinsic oscillatory frequencies of the neurons, we show that through spike-timing-dependent plasticity the synapses which have the high-frequency neurons as presynaptic tend to be potentiated while the links originated from the low-frequency neurons are weakened. The emergent effective flow of directed connections introduces the high-frequency neurons as the more influential elements in the network and facilitates synchronization by decreasing the synaptic cost for onset of synchronization.

DOI: 10.1103/PhysRevE.86.011925 PACS number(s): 87.19.lm, 87.19.lw

Experimental studies indicate that excitatory synapses are very sensitive to the temporal order of firing of pre- and postsynaptic neurons [1]. Spike-timing-dependent plasticity (STDP) dictates that synaptic efficacy increases if firing of a presynaptic neuron occurs in advance of firing of a postsynaptic neuron, and decreases if the temporal order of firing is reversed [1,2]. Indeed, STDP is widely thought to underlie learning processes, and in itself constitutes a broadly interesting phenomenon [3,4].

Many studies on synchronization both at the scale of a few neurons and in large networks reveal that with STDP neural synchronization is more rapid and robust [5]. Compared to networks of fixed coupling strength, in the networks in which the couplings change according to STDP, the regions of synchronization in the parameter space are wider; e.g., they can suffer larger mismatch in intrinsic frequencies yet show synchronized behavior.

While most of the early studies on synchronization properties of complex networks ignore the evolution of network structure and the directionality of the links, recent studies address both the effect of the links' directionality [6–9] and time-dependent coupling strengths [10]. When networks are directed, the Jacobian or Laplacian matrices will have complex eigenvalues that influence both the stability [11] and the dynamical organization of complex networks [6,9]. Here we study how STDP changes the structure of the directional links of a neuronal network, in an initially (topologically) homogeneous network consisting of nonidentical oscillators. Starting with an all-to-all network with symmetric couplings, we will show that disorder in the intrinsic oscillatory frequencies leads to asymmetric couplings in a predictable manner; i.e., the evolution of the network is such that the influence of the neurons (strength of outgoing couplings) with higher rate of activity is enhanced and in turn, the strength of incoming coupling to the neurons with lower rate of activity is increased. We also show that the coupling cost for the onset of synchronization for such a network, which has an effective network flow of the directed connections from high-frequency to low-frequency components, is smaller than that of a symmetric network [9]. So in a network of constant sum of the node strengths, such effective flow of connections leads to more organized dynamics. In turn we show that the evolution of the synaptic strengths in the network depends on whether or not synchrony is achieved through STDP.

The model network consists of N pulse-coupled leaky integrate-and-fire (LIF) oscillators, each of them defined by a linear first-order equation

$$C\frac{dV_i}{dt} = -g_l(V_i - V_l) + J_i + \sum_j J_{ij}, \tag{1}$$

in which V_i is the membrane voltage for each neuron labeled by $i = 1,2,...,N$. C is the membrane capacitance, J_i is the external current, and J_{ij} is synaptic current with the neurons j and i as the pre- and postsynaptic neurons, respectively. g_l is the leak conductance and V_l the resting potential. Assuming a threshold voltage V_{th} for spike generation, after dividing both sides by $J_0 = g_l(V_{th} - V_l)$ and defining dimensionless voltage $v = (V - V_l)/(V_{th} - V_l)$, we get

$$\frac{dv_i}{d\tau} = -v_i + I_i + \sum_j I_{ij}, \tag{2}$$

where $\tau = t/\tau_0$ is dimensionless time in the units of the membrane time constant $\tau_0 = C/g_l$. $I_i = J_i/J_0$ and $I_{ij} = J_{ij}/J_0$ are dimensionless external and synaptic currents, respectively. In the normalized units every time a threshold value $v_{th} = 1$ is reached, the neuron *fires* and the voltage resets to $v_{res} = 0$. The voltage of an isolated LIF neuron with constant input current oscillates with the period $T = \ln[I/(I - v_{th})]$. The spikes are recorded by the *neuron's response function* [12] defined as $x_i(t) = \sum_m \delta(t - t_i^m)$ where t_i^m is the time of mth firing of the neuron i and $\delta(x)$ is the Kronecker delta function. The synaptic current I_{ij} is defined as

$$I_{ij} = a_{ij}g_{ij}x_j(t), \tag{3}$$

where a_{ij} is the element of the adjacency matrix [13] which is one when there is a direct connection between the neurons i and j as the pre- and postsynaptic neurons and zero otherwise. Synaptic strength g_{ij} is positive throughout this study to model excitatory synapses. For later convenience we call the matrix formed by the elements $a_{ij}g_{ij}$ the *weighted adjacency matrix*.

In this minimal model where all the neurons have the same time constant, inhomogeneity in the intrinsic rates of activity is imposed by unequal external currents; e.g., the

currents I_i can be chosen from a distribution. So throughout the paper we call the neurons with larger feed high-frequency neurons, and the neurons with smaller feed low-frequency neurons. The distribution of the oscillatory frequencies can be calculated using the relation of the oscillatory frequency of a LIF neuron to input current as $r = \{\ln[I/(I - v_{th})]\}^{-1}$. Note that inhomogeneity could also be imposed by choosing neurons with different time constants and equal feeds.

The time-dependent synaptic coupling strength g_{ij} changes depending on the dynamics of the presynaptic and postsynaptic neurons. Through additive STDP g_{ij} changes by Δg_{ij}, which is independent of the current value of g_{ij} and is a function of the time difference $\Delta t = t_i - t_j$ between the times of postsynaptic and presynaptic spikes. Synaptic modification Δg_{ij} is provided by

$$\Delta g_{ij} = A_{\pm}\mathrm{sgn}(\Delta t)\exp(-|\Delta t|/\tau_{\pm}), \tag{4}$$

where $\mathrm{sgn}(x)$ is the sign function. The parameters τ_+ and τ_- determine the ranges of pre-to-postsynaptic interspike intervals over which synaptic strengthening and weakening occurs. A_+ and A_-, which are both positive, determine the maximum amounts of synaptic modification which occur when Δt is close to zero [2]. A_+ (A_-) and τ_+ (τ_-) are used when Δt is positive (negative). Divergence of the synaptic strengths is prevented by assuming limiting values for the synaptic strength.

It was noted by Gilson *et al*. that symmetry of the coupling matrix is broken by STDP [14,15]. We study the possible effect of such asymmetry on the dynamics of the network and how the dynamics in turn affects the structure of the connections in the network. We first define the *synaptic cost* as the sum of all synaptic strengths in the array $G = \sum_{i,j} a_{ij} g_{ij}$. To quantify the asymmetry, we define *link imbalance* as the difference of the synaptic strengths between two nodes $C_{ij} = -C_{ji} = a_{ij}g_{ij} - a_{ji}g_{ji}$. Furthermore, we introduce the *strength* of node i as the sum of all the outgoing synaptic strengths, i.e., the synapses which have the neuron i as presynaptic $C_i^+ = \sum_j a_{ji}g_{ji}$, and *sensitivity* of the node as the incoming synaptic strengths, the synapses which have the neuron i as postsynaptic $C_i^- = \sum_j a_{ij}g_{ij}$. These sums can also be interpreted as the sum of the elements of the ith column and ith row of the weighted adjacency matrix, respectively. We call the difference between the outgoing and incoming synaptic strengths for each neuron $C_j = C_j^+ - C_j^-$ the *node imbalance*. A positive node imbalance means the neuron's outgoing synapses are stronger than its incoming synapses and vice versa. Also to quantify effective imbalance in the network we introduce *network imbalance* as $C_{\mathrm{net}} = 1/G \sum_{i,j} \mathrm{sgn}(j - i)g_{ij}$ with G being the synaptic cost. In this sum all the synapses with $j > i$, i.e., those for which the index of the presynaptic neuron is larger than the postsynaptic one, are considered with positive weight and vice versa. These two groups of synapses are shown in Fig. 1. In the extreme cases when all the backward (forward) links are set to zero, network imbalance is 1 (-1) and nonzero intermediate values of network imbalance indicate an effective imbalance in the forward and backward synaptic strengths. Note that when all the link imbalances are zero the network imbalance is also zero but the inverse is not true since C_{net} is averaged on all the link imbalances. In the following we first inspect the effect of predetermined network imbalance on the dynamic of a network with static synapses and then we will show that STDP can change network imbalance in a predictable manner.

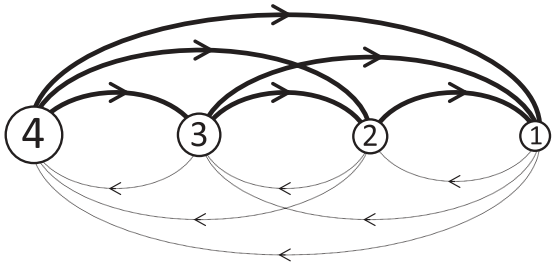

FIG. 1. The model network with 4 neurons. The forward synaptic links, those which have a node with larger index as presynaptic and a node with smaller index as the postsynaptic neuron, are shown by thick lines. Thin lines show the backward links with reverse definition.

We construct a fully connected network without self-connections ($a_{ij} = 1$ for $i \neq j$ and zero for $i = j$) and we vary the link imbalances by assuming the synaptic strengths as $g_{ij} = 1/N[g_0 + \eta\ \mathrm{sgn}(j - i)f(|j - i|)]$ with constant g_0 and $f(\xi)$ a monotonically increasing function of ξ. Then the link imbalance $C_{ij} = 2\eta\ \mathrm{sgn}(j - i)f(|j - i|)$ and the network imbalance $C_{\mathrm{net}} = \eta/(NG)\sum_{i,j} \mathrm{sgn}(j - i)f(|j - i|)$ can be controlled by the parameter η. With $\eta = 0$ all the links and the network are balanced. Positive η constructs a network in which nodes with larger index have larger strength and vice versa. Please note that synaptic cost for the network remains constant (equal to g_0) when changing the imbalance parameter η. Finally, we choose the external currents equally spaced in the interval $[I_0 - \delta, I_0 + \delta]$, and label the neurons in order of increasing input current, i.e., the $j = 1$ neuron has the smallest input and so on.

Now we inspect how the dynamics of the network are affected by changing the imbalance parameter η. The *network activity* is defined as the average response function of all the neurons in the array $X_{\mathrm{net}}(t) = 1/N \sum_i x_i(t)$. In-phase (periodic) firing of a large fraction of neurons in the array leads to oscillatory behavior of the network activity function with large amplitude, so the amplitude of the oscillation of the network activity function can be used as an order parameter showing how synchronized the firing of the neurons in the network are. In Fig. 2(a) we have shown how the order parameter changes when we increase the imbalance parameter in a network with a constant synaptic cost. The plots show that the degree of synchronization can be elevated when we increase the strength of high-frequency neurons and decrease their sensitivity [see also Figs. 2(b) and 2(c)]. It is also shown that a negative network imbalance has no effect on the coherence of the behavior of the neurons; i.e., they are outgoing synapses from the high-frequency neurons which should be strengthened to achieve synchrony. It is also shown in the inset of Fig. 2(a) that mean frequency of the array increases with the imbalance parameter, which is a reasonable consequence of the increase of the strength of high-frequency neurons. In such a system (when all the synapses are excitatory) increase in the strength of the high-frequency components (while the sensitivity of the low-frequency components increases as well)

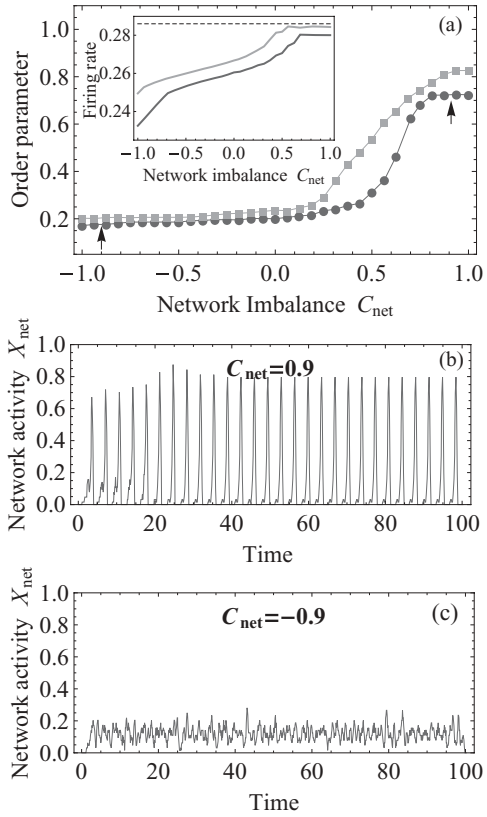

FIG. 2. (a) The order parameter, the average amplitude of the network activity (see below) as a function of network imbalance, C_{net}. In a network of $N = 64$ neurons with all-to-all connections, input currents are chosen as $I_j = 1 + 0.0005j$ and synaptic strengths as $g_{ij} = 1/N[g_0 + \eta\ \mathrm{sgn}(j-i)f(|j-i|)]$ with $f(x) = \tanh(2x)$. The results are shown for $g_0 = 0.03$ (black circles) and $g_0 = 0.04$ (gray squares). Corresponding range of η for each value of g_0 is chosen such that all the synaptic strengths are nonnegative. Increasing η beyond this range results in negative synaptic strengths which we do not consider here. To calculate the order parameter in each trial, after discarding 50 time units as transient, we have recorded maximum and minimum values of the network activity $X_{net}(t)$ for every 10 time units. The amplitude (difference between maximum and minimum) is then averaged over 100 trials each containing 100 intervals. Finally we have normalized the results by the maximum value of the response function of a single neuron. In (b) and (c) the normalized network activity, $X_{net}(t)$, is shown for two different values of the imbalance parameter η depicted by arrows in (a); periodic behavior of the network activity with relatively large amplitude in (b) indicates synchrony of the neurons. Inset of (a) shows mean frequency of the neurons in the network vs network imbalance for $g_0 = 0.03$ (black line) and $g_0 = 0.04$ (gray line). Dashed line in the inset shows the oscillatory frequency of the neuron with the highest intrinsic frequency in the network.

leads to increase of both the mean frequency of the network and the degree of synchrony.

We now let the synaptic strengths evolve through STDP. We show that dependent on initial synaptic strengths, STDP may lead to organized dynamics in the network and this in turn affects the emergent structure of the network. Again we consider a fully connected network with initially equal symmetric synaptic strengths. We assume an antisymmetric STDP profile with usual criteria ($A_+ > A_-$ and $A_+\tau_+ < A_-\tau_-$) and zero lower cutoff for g_{ij}. We examine two situations; in both cases the initial synaptic strengths are not enough to overcome disorder in the array and the neurons are unsynchronized when STDP is absent. Asymmetry induced by STDP in one of the experiments leads to synchrony whereas in the second experiment the neurons remain unsynchronized in the steady state as is shown in Figs. 3 and 4.

When STDP leads to synchronized firing of the neurons (Fig. 3), a net synaptic flow is constructed from the high-frequency neurons to the low-frequency ones, which is reflected in the value of network imbalance as it takes a relatively large positive value ($C_{net} \simeq 0.8$) in the steady state. The large positive network imbalance indicates almost all of the weakened synapses are those from low-frequency to high-frequency neurons and those which are strengthened are from high-frequency neurons to low-frequency ones. We note that asymmetry induced by STDP is in agreement with previous studies [15], but here with the differences in intrinsic rate of firing of the neurons, one can predict which synapses are more likely to be strengthened and which synapses are to be weakened. With the parameters we have chosen the synaptic cost of the network decreases; this is of great importance since synchrony can be achieved in spite of such a decrement in the synaptic cost. This is consistent with the results demonstrated in Fig. 2 which indicates positive network imbalance lowers the synaptic cost for onset of synchronization. Both the evolution of the synaptic cost and final coherence of the network dynamics are dependent on the choice of the ratio $\gamma = (A_+\tau_+)/(A_-\tau_-)$. To check this, we increased γ from 0.5 to 1 in increments of 0.01. With $\gamma \gtrsim 0.7$ the neurons show coherent behavior in the steady state and they will be more synchronized if we increase γ further. With $\gamma \gtrsim 0.8$ synaptic cost also increases but nevertheless network imbalance increases in all the range of γ which we tested.

Emergent structure and the coherence of the dynamics in the steady state also depend on the choice of the initial synaptic weights. With smaller values of the initial synaptic strengths, synchrony can be achieved by choosing larger values for parameter γ (while keeping all the other parameters unchanged). In an experiment with the same parameters of Fig. 3, we have lowered the initial synaptic weights and the plasticity has not led the neurons to synchrony (Fig. 4). In this case the time course of the network imbalance is dependent on the initial conditions but in all the trials final value of network imbalance is a relatively small positive value (about 0.2).

As noted above, positive network imbalance increases mean frequency of the network since the mean excitation grows with increasing strength of the high-frequency neurons. In the presence of STDP this effect competes with the possible decrease in synaptic cost which naturally decreases the mean frequency. The increase in the oscillatory frequency seen in Fig. 3(f) shows that the former effect has been overcome, but the change is less than 4% which shows that the effect of the imbalance has been mainly canceled by the decrease in the synaptic cost. Note that in the inset of Fig. 2(a) where the synaptic cost has been kept constant, increase in frequency amounts to 15%. Since the final value of the mean frequency

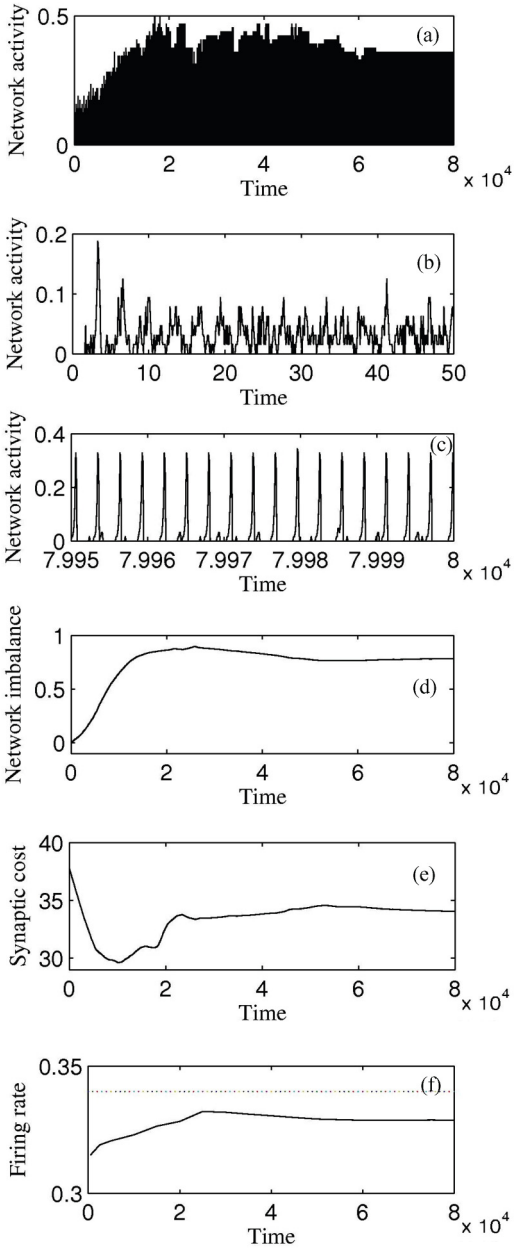

FIG. 3. (Color online) In (a) the network activity $X_{\text{net}}(t)$ is shown when the synaptic strengths evolve through STDP. The boosted amplitude of activity is due to transition of the network to an oscillatory state which indicates synchrony in the array. This has been clarified in (b) and (c) where the network activity is shown at a magnified time scale in the initial transient state and in the final steady state, respectively. In (d) evolution of the network imbalance C_{net} is shown. In (e) and (f) the evolution of the synaptic cost G and mean frequency of the neurons are shown, respectively. Network imbalance in each time step is normalized by instantaneous value of synaptic cost G. Mean oscillatory frequencies is calculated in windows of duration 500 time units and then normalized by number of neurons in the network. Dotted line in (f) shows the oscillatory frequency of the neuron with the highest intrinsic frequency. The currents are chosen as $I_i = 1 + 0.001i$; lower and upper cutoffs are zero and $0.12/N$, respectively. The network size is $N = 64$ and the initial couplings are all equal to $0.06/N$ which gives the initial value for synaptic cost $G(0) = 38.4$. Parameters of STDP are $A_+ = 10^{-5}$ nS, $A_- = 0.9 \times 10^{-6}$ nS, $\tau_+ = 10$ ms, and $\tau_- = 15$ ms.

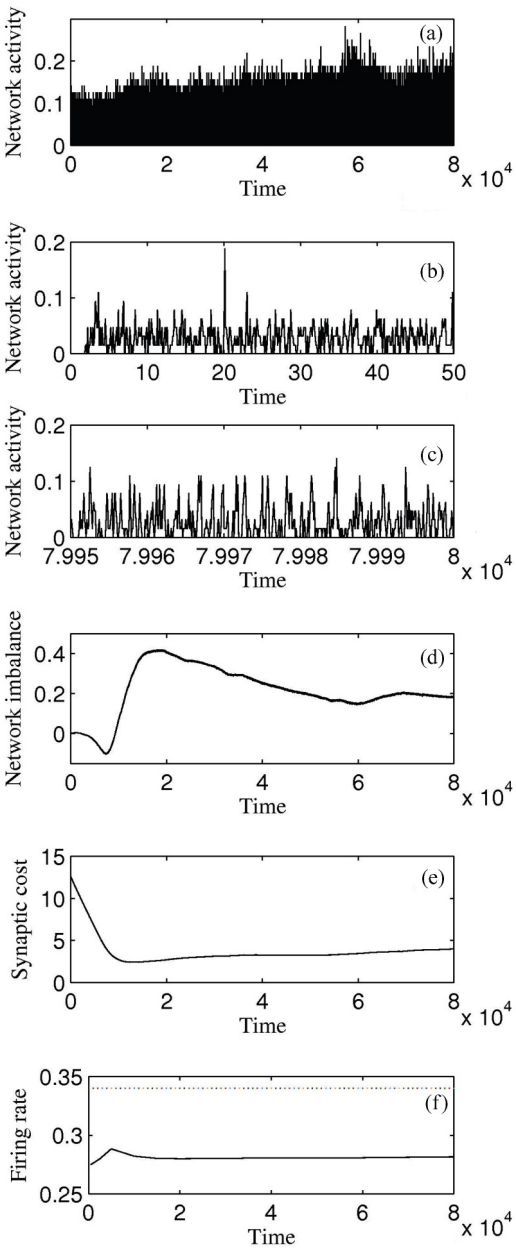

FIG. 4. (Color online) In (a) the network activity is shown when the synaptic strengths evolve through STDP for the same network as in Fig. 3 with smaller initial synaptic strengths. All the parameters are the same as in Fig. 3 except for the initial couplings which here are all equal to $0.02/N$ which gives the initial synaptic cost $G(0) = 12.8$. Plots (b) and (c) show the network activity in two different time ranges at a magnified time scale. In (d) evolution of the network imbalance C_{net} is shown. In (e) and (f) the evolution of the synaptic cost G and mean oscillatory frequency of the neurons are shown, respectively. Dotted line in (f) shows the oscillatory frequency of the neuron with the highest intrinsic frequency in the network.

depends on the evolution of both synaptic cost and network imbalance, it is affected by the ratio γ and the initial synaptic weights. As is seen in Fig. 4, the effects of network imbalance and synaptic cost may cancel each other leaving the oscillatory frequency almost equal to its initial value.

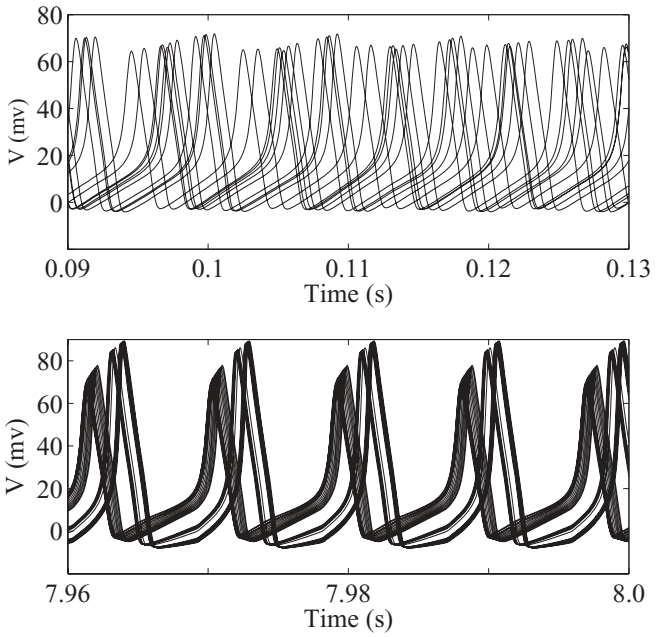

FIG. 5. Membrane voltages of the sample neurons are given at two different times in the initial state (upper plot) and at steady state (lower plot). The parameters of the HH neurons and synapses are given in the Appendix. Other parameters are $A_+ = 9$ nS, $A_- = 8.6$ nS, $\tau_+ = 20$ ms, and $\tau_- = 30$ ms.

We have repeated a similar experiment using Hodgkin-Huxley neurons with conductance-based synapses (see Appendix), to assess whether the results are applicable in the more biologically plausible models. As shown in Fig. 5, the role of STDP is to decrease the effect of the discrepancy on the intrinsic frequencies and organize the dynamics of the neurons. In turn, the emergent structure of the network is shown in Fig. 6

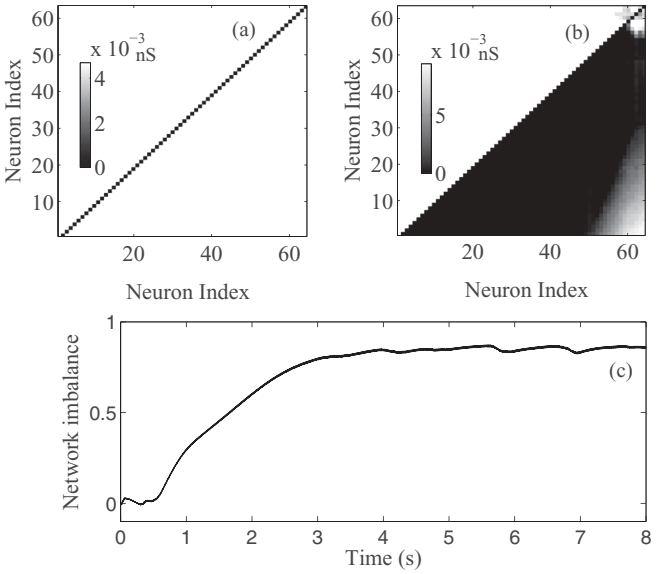

FIG. 6. In a network composed of 64 Hodgkin-Huxely neurons connected with conductance-based synapses, the initially symmetric weighted adjacency matrix (a) evolves to a nearly triangular matrix in the steady state (b). In (c) the evolution of network imbalance is shown. All the parameters are those of Fig. 5.

where a nearly triangular weighted adjacency matrix is formed and network imbalance is reasonably increased.

In passing, to ascertain the effect of imbalance on the synchronization of coupled neurons, we show that for two weakly connected nonidentical neurons with excitatory couplings, both increasing the strength of the high-frequency neuron and decreasing its sensitivity extend the domain of synchronization and lower the threshold synaptic cost for the onset of synchronization. We consider two neurons with the inputs $I_2 = I_1 + \delta$ which are connected by two directed couplings with the strengths g_{12} and g_{21}. With positive mismatch parameter $\delta > 0$ the second neuron spikes with a higher rate. Looking for an existence criterion for the in-phase $1:1$ synchronization, we consider the two cases in which one of the neurons (master) fires and makes also the other neuron (slave) fire. In the first case we assume the high-frequency neuron first fires at time t_i and the low-frequency neuron fires just after it; i.e., the high-frequency neuron is the master and the low-frequency neuron is the slave. With no refractory period, firing of the slave neuron changes the voltage of the master by g_{21} and the high-frequency neuron would fire again at time $t_{i+1} = t_i + \ln(\frac{I_2 - g_{21}}{I_2 - 1})$. Firing of the master neuron raises the voltage of the slave by g_{12}, and if at the time of the firing of the master t_{i+1} the voltage of the slave neuron is larger than $1 - g_{12}$, the voltage of the slave exceeds the threshold and it would fire just after the master neuron. This means the neurons fire synchronously. The voltage of the slave neuron at t_{i+1} is $v_1(t_{i+1}) = I_1\{1 - \exp[-(t_{i+1} - t_i)]\}$ and the above criterion for in-phase firing $v_1(t_{i+1}) > 1 - g_{12}$ leads to

$$I_1 > (1 - g_{12})\frac{I_2 - g_{21}}{1 - g_{21}}. \tag{5}$$

With $\delta = I_2 - I_1$ we have

$$\delta < I_2 - (1 - g_{12})\frac{I_2 - g_{21}}{1 - g_{21}}. \tag{6}$$

With fixed I_2 this equation determines the domain of synchronization, the maximum mismatch which the system can suffer and yet the neurons fire synchronously. Interestingly, increasing the forward coupling g_{21} broadens the domain of synchronization while backward coupling shrinks this domain. Since we have assumed here that the slave neuron is the low-frequency one, it cannot exceed the high-frequency neuron and the above equation solely determines the existence condition for the in-phase solution. The second case, which as we will see is possible for large values of coupling constants, assumes that the low-frequency neuron is the master. In this case a criterion similar to Eq. (5) exists and also we should prevent the high-frequency neuron's potential from exceeding the low-frequency neuron's potential; i.e., at the time of next firing of the master neuron t_{i+1} the voltage of the high-frequency neuron should be less than threshold. Combining these expressions we have

$$I_2 - \frac{I_1 - g_{12}}{1 - g_{12}} < \delta < I_2 - (1 - g_{21})\frac{I_1 - g_{12}}{1 - g_{12}}. \tag{7}$$

In the equations above two points are worth noting: For small values of the coupling, which is the case of our study, just the synchronized state with the high-frequency neuron

as the master can exist and this state is destabilized by increasing strength of the outgoing synaptic conductance of the low-frequency neuron g_{21}. In other words, for small values of synaptic strengths (where the only possible in-phase state is the state with the high-frequency neuron as the master), g_{12} increases synchrony and g_{21} opposes it. Although it can be shown for near-threshold currents $I_i \sim 1 + O(\epsilon)$ and small synaptic strengths $g_{ij} \sim O(\epsilon)$ that the effect of g_{21} is of order ϵ^2, for larger input currents the effect of the strength of the low-frequency neuron can be comparable with that of the high-frequency neuron. With STDP for two weakly connected neurons, our results show that the strength of the high-frequency neuron always increases and that of the low-frequency neuron decreases, and as noted above both of them enhance synchrony. When synchrony is achieved (with the high-frequency neuron as the master), the rate of change of the synaptic strengths increases and then they are just limited by the cutoffs imposed on synaptic weights.

To conclude, we have shown that in systems of weakly connected neurons with excitatory synapses, when there is a mismatch in the intrinsic oscillatory frequencies of neurons, an asymmetric arrangement of synaptic constants can enhance synchrony. In this arrangement directed links from the high-frequency elements to the low-frequency ones should be stronger. In a two-neuron system, this result is verified by a simple analytic reasoning. We have also shown that spike-timing-dependent plasticity in disordered networks can organize the firing of the neurons by imposing such asymmetry on the matrix of synaptic strengths. While synchrony enhanced by STDP has been reported before, here we proposed that this effect can be related to the asymmetric rearrangement of the synaptic couplings in the disordered neuronal ensembles.

To construct a single framework for different types of plasticity [16], it will be interesting to know how STDP at a given synapse builds up over time. This can shed light on the relationship between STDP and different forms of rate-coded models of plasticity, e.g., the BCM model [17]. Our findings suggest that in the presence of disorder, the cumulative effect of STDP for the synapses depends on the comparative values of the oscillatory frequencies of the pre- and postsynaptic neurons. In this regard our results are in line with the results reported by Izhkevich and Desai [18] for the correlated spike trains. Assuming a fixed postsynaptic frequency we have shown that high presynaptic oscillating frequencies result in potentiation while low frequencies lead to depression.

Most investigations have explored STDP in excitatory synapses, though a small subset has addressed the issue of plasticity at inhibitory synapses [19]. Throughout the brain, inhibitory synapses serve both to modulate excitation in principal neurons and to regulate rhythmic circuits [20,21]. Modeling studies have suggested potential functions for plastic inhibition in circuit rhythm generation [22] and in balancing excitation [23]. It remains to be checked whether our results on the functional and structural effects of STDP in disordered networks are applicable in more biologically plausible arrangements, e.g., in the presence of static and plastic inhibitory synapses.

The authors gratefully acknowledge Tom Tetzlaff and F. Ghaffar for reading the manuscript and giving useful comments.

APPENDIX: THE HODGKIN-HUXLEY MODEL AND CONDUCTANCE-BASED SYNAPSES

The membrane voltage of the neuron in the Hodgkin-Huxley (HH) model is described by [24]

$$c\frac{dv_i}{dt} + I_{na} + I_k + I_l + I_{ij} = I_i. \tag{A1}$$

c is the capacitance per unit area of the membrane which is taken as 1 μF/cm^2 and I_j stands for the external current. $I_l = g_l(v_j - E_l)$ is the passive leak current and $I_{na} = g_{na}m^3h(v_j - E_{na})$ and $I_k = g_k n^4(v_j - E_k)$ are sodium and potassium currents, respectively. $g_l = 0.3$ mS/cm^2 is the conductance for the leak current and $g_{na} = 120$ mS/cm^2 and $g_k = 36$ mS/cm^2 are the maximum conductance for the sodium and potassium ions, and $E_l = 10.6$ mV, $E_{na} = 115$ mV, and $E_k = -12$ mV are reversal voltages for the leak, sodium, and potassium currents, respectively. m_j (h_j), the activation (inactivation) variable of sodium, and n_j, the activation variable of potassium, obey the differential equations

$$\begin{aligned}\frac{dm_j}{dt} &= \alpha_m(1 - m_j) - \beta_m m_j,\\ \frac{dh_j}{dt} &= \alpha_h(1 - h_j) - \beta_h h_j,\\ \frac{dn_j}{dt} &= \alpha_n(1 - n_j) - \beta_n n_j,\end{aligned} \tag{A2}$$

where α and β are functions of membrane voltage that can be found in [24].

With conductance-based synapses the synaptic current is described by $I_{ij} = a_{ij}\bar{g}_{ij}s_{ij}(t - \tau)(v_i - E_{syn})$ where $\bar{g}_{ij}$ is the synaptic maximum conductivity and E_{syn} is the synaptic reversal potential. $s_{ij}(t)$ is the synaptic activity function defined via

$$\frac{ds_{ij}}{dt} = \alpha_s f(v_j - v_{th})(1 - s_{ij}) - \beta_s s_{ij}, \tag{A3}$$

with α_s and β_s defining the activation and deactivation time constants, $v_{th} = 20$ mV is the threshold voltage for the activation of the synapse, and f is the threshold function $f(x) = 1/2[1 + \tanh(5x)]$.

The parameters we have chosen are such that with $I_{\text{ext}} = 0$, the resting potential of the neuron is zero; so the choice $E_{syn} = 80$ mV is reasonable for excitatory neurons. Inspired by typical time constants of the activation and deactivation of excitatory synapses with AMPA receptors, we have chosen $\alpha_s = 10$ ms^{-1} and $\beta_s = 0.5$ ms^{-1} as the activation and deactivation time constants for fast synapses [25].

[1] H. Markram, J. Lübke, M. Frotscher, and B. Sakmann, Science **275**, 213 (1997); L. I. Zhang *et al*., Nature (London) **395**, 37 (1998); G. Q. Bi and M.-M. Poo, J. Neurosci. **18**, 10464 (1998); Annu. Rev. Neurosci. **24**, 139 (2001); J. P. Pfister and W. Gerstner, J. Neurosci. **26**, 9673 (2006).

[2] S. Song, K. D. Miller, and L. F. Abbott, Nat. Neurosci. **3**, 919 (2000); M. C. W. van Rossum and G. G. Turrigiano, Neurocomputing **38-40**, 409 (2001); A. Morrison, M. Diesmann, and W. Gerstner, Biol. Cybern. **98**, 459 (2008).

[3] C. Leibold, A. Gundlfinger, R. Schmidt, K. Thurley, D. Schmitz, and R. Kempter, Proc. Natl. Acad. Sci. USA **105**, 4417 (2008); S. S. Talathi, H. D. I. Abarbanel, and W. L. Ditto, Phys. Rev. E **78**, 031918 (2008); T. Voegtlin, Neural Comput. **21**, 1749 (2009); T. Masquelier, R. Guyonneau, and S. J. Thorpe, *ibid.* **21**, 1259 (2008); P. D'Souza, S.-C. Liu, and R. H. R. Hahnloser, Proc. Natl. Acad. Sci. USA **107**, 4722 (2009); M. Gilson, A. N. Burkitt, D. B. Grayden, D. A. Thomas, and J. L. van Hemmen, Phys. Rev. E **82**, 021912 (2010).

[4] R. Kempter, W. Gerstner, and J. L. van Hemmen, Phys. Rev. E **59**, 4498 (1999).

[5] V. P. Zhigulin, M. I. Rabinovich, R. Huerta, and H. D. I. Abarbanel, Phys. Rev. E **67**, 021901 (2003); J. Karbowski and G. B. Ermentrout, *ibid*. **65**, 031902 (2002); T. Nowotny, V. P. Zhigulin, A. I. Selverston, H. D. I. Abarbanel, and M. I. Rabinovich, J. Neurosci. **23**, 9776 (2003).

[6] J. G. Restrepo, E. Ott, and B. R. Hunt, Chaos **16**, 015107 (2005).

[7] S. M. Park and B. J. Kim, Phys. Rev. E **74**, 026114 (2006); G. Zamora-Loez, V. Zlatić, C. Zhou, H. Štefancić, and J. Kurths, *ibid*. **77**, 016106 (2008).

[8] G. Bianconi, N. Gulbahce, and A. E. Motter, Phys. Rev. Lett. **100**, 118701 (2008).

[9] T. Nishikawa and A. E. Motter, Phys. Rev. E **73**, 065106(R) (2006); Physica D **224**, 77 (2006).

[10] J. Ito and K. Kaneko, Phys. Rev. Lett. **88**, 028701 (2001); M. Porfiri, D. J. Stilwell, and E. M. Bollt, IEEE Trans. Circuits Syst. **55**, 3170 (2008); I. Belykh, V. Belykh, and M. Hasler, Physica D **224**, 42 (2006).

[11] M. R. Gardner and W. R. Ashby, Nature (London) **228**, 784 (1970); R. M. May, *ibid*. **238**, 413 (1972).

[12] P. Dayan and L. F. Abbot, *Theoretical Neuroscience: Computational and Mathematical Modeling of Neural Systems* (MIT Press, 2001).

[13] R. Albert and A.-L. Barabási, Rev. Mod. Phys. **74**, 47 (2002).

[14] M. Gilson, A. N. Burkitt, D. B. Grayden, D. A. Thomas, and J. L. van Hemmen, Biol. Cybern. **101**, 81 (2009).

[15] M. Gilson, A. N. Burkitt, D. B. Grayden, D. A. Thomas, and J. L. van Hemmen, Biol. Cybern. **101**, 411 (2009).

[16] H. Z. Shouval, S. S.-H. Wang, and G. M. Wittenberg, Front. Comput. Neurosci. **4**, 19 (2010).

[17] E. L. Bienenstock, L. N. Cooper, and P. W. Munro, J. Neurosci. **2**, 32 (1982).

[18] E. M. Izhikevich and N. S. Desai, Neural Comput. **15**, 1511 (2003).

[19] J. S. Haas, T. Nowotny, and H. D. I. Abarbanel, J. Neurophysiol. **96**, 3305 (2006).

[20] C. A. van Vreeswijk and H. Sompolinsky, Science **274**, 1724 (1996).

[21] W. W. Lytton and T. J. Sejnowski, J. Neurophysiol. **66**, 1059 (1991); X.-J. Wang and G. Buzsáki, J. Neurosci. **16**, 6402 (1996).

[22] C. Soto-Trevino, K. A. Thoroughman, E. Marder, and L. F. Abbott, Nat. Neurosci. **4**, 297 (2001).

[23] C. P. Marder and D. V. Buonomano, J. Neurosci. **24**, 8873 (2004); T. P. Vogels, H. Sprekeler, F. Zenke, C. Clopath, and W. Gerstner, Science **334**, 1569 (2011).

[24] A. L. Hodgkin and A. F. Huxley, J. Physiol. **117**, 500 (1952).

[25] W. Gerstner and W. M. Kistler, *Spiking Neuron Models* (Cambridge University Press, 2002).